Flow Properties of Submerged Heated Effluents in a Waterway

JAMES F. CAMPBELL*
NASA Langley Research Center, Hampton, Va.

AND

JOSEPH A. SCHETZ†
Virginia Polytechnic Institute and State University, Blacksburg, Va.

An experimental and theoretical investigation has been undertaken to study the trajectory and growth of thermal effluents having a range of discharge velocities and temperatures. The discharge of an effluent into a waterway was mathematically modeled as a submerged jet injection process by using an integral method which accounts for natural fluid mechanisms such as turbulence, entrainment, buoyancy, and heat transfer. The analytical results are supported by experimental data and demonstrate the usefulness of the theory for estimating the location and size of the effluent with respect to the discharge point. The capability of predicting jet flow properties, as well as the jet path, was enhanced by obtaining the jet cross-sectional area during the solution of the conservation equations (a number of previous studies assume a specific growth for the area). Realistic estimates of temperature in the effluent were acquired by accounting for heat losses in the jet flow due to forced convection and to entrainment of freestream fluid into the jet.

Nomenclature

A = cross-sectional area of jet control volume
b = width of turbulent mixing zone
C = effective jet circumference
C_D = drag coefficient $(D/q_{\infty_n} S)$
C_p = pressure coefficient $[(p-p_\infty)/q_{\infty_n}]$
D = drag force on jet flow due to blockage of freestream flow
d = effective jet diameter
ds = infinitesimal length of jet control volume
E = entrained mass flow per unit of jet length
E^* = entrainment coefficient
F = constant in expression for Nu_d, see Eq. (17)
g = gravity
h = width of jet flow
$\bar{h}$ = average film heat-transfer coefficient
k = thermal conductivity of jet fluid
m = mass of jet fluid in control volume
m_e = freestream mass entrained into jet control volume
Nu_d = Nusselt number based on $d(\bar{h}d/k)$
Pr = Prandtl number
p = local static pressure around perimeter of jet cross section
p_∞ = freestream static pressure
$\bar{p}$ = average static pressure in jet flow
Q = rate of heat flow from jet fluid
q = dynamic pressure of jet flow $(\rho v^2/2)$
q_∞ = dynamic pressure of freestream flow $(\rho_\infty v_\infty^2/2)$
R = radius of curvature of jet trajectory $(d\alpha/ds)^{1/2}$
Re_d = Reynolds number based on d
S = frontal area of jet control volume $(h\,ds)$
s,n = natural coordinates along and perpendicular to jet trajectory
T = average temperature of jet fluid
T_∞ = freestream temperature
VR = effective velocity ratio, $[(\rho v^2)_i/(\rho v^2)_\infty]^{1/2}$
v = average velocity of jet fluid
v_∞ = freestream velocity
x,y = Cartesian coordinates
α = inclination of jet axis
β = constant in expression for ε, see Eq. (9)
γ = constant in expression for Nu_d, see Eq. (17)
ε = virtual kinematic (eddy) viscosity
θ = angular orientation of p
λ = velocity parameter in expression for β, see Eq. (14)
ν = kinematic viscosity
ρ = average density of jet fluid
ρ_∞ = freestream density
τ = shear stress in s direction acting on jet flow

Subscripts

i = jet flow conditions at injection point
max = maximum
min = minimum
n = condition in n direction
1,2 = jet flow conditions in control volume before and after entrainment

Presented as Paper 72-79 at the 10th Aerospace Sciences Meeting, San Diego, Calif., January 17–19, 1972; submitted February 24, 1972; revision received July 17, 1972. This work was supported in part by the Office of Water Resources Research under Grant B-041-VA.

Index categories: Jets, Wakes, and Viscid-Inviscid Flow Interactions; Viscous Nonboundary-Layer Flows.

* Aerospace Engineer. Associate Fellow AIAA.

† Chairman, Aerospace Engineering Department. Associate Fellow AIAA.

Introduction

ONE area in which aerospace technology can be applied to alleviate environmental problems is in understanding and monitoring the dispersion of a polluted effluent discharged into a water system. This includes the thermal pollution problem where a degrading effect on the local water environment may occur because of continual discharge of large volumes of heated water.

Some of the previous studies directed toward the physical understanding of the thermal pollution problem have been more concerned with the far-field effects of a thermal discharge, such as the overall heat balance of bodies of water having heat addition,[1] or the diffusion of water temperature assuming a one- or two-dimensional mixing model.[2] However, since it is desirable to observe the time history of a heated effluent from the point of discharge to the point of final thermal mixing with the ambient fluid, it is therefore necessary to consider the near-field effects. This is certainly the more pragmatic approach to the physical understanding of the problem, particularly if the definition of a thermal "mixing zone" is desired in order to minimize impact on the local water environment.

Fig. 1 Photographs of side view of vertical injection for several injection velocities; $T_i = T_\infty$.

The near-field region of a submerged effluent discharged into a moving water environment is often modeled as a turbulent jet injection process and has been examined by a number of experimental[3-7] and theoretical[8-11] research studies. The purpose of the present investigation is to extend the results of these previous experimental studies, and to develop a theory that provides improved predictions of jet trajectory along with estimates of jet flow properties.

Experiment

The experimental portion of the present investigation was conducted in a water channel using city water which was clear, bubble free, and at room temperature. The injection process in the channel was documented with photographs taken simultaneously with cameras located above and to the side of the channel. The apparatus used during the tests is briefly described in the following sections, whereas complete details are presented in Ref. 12.

Main-Flow Channel

The main-flow channel was a modified Hydraulic Demonstration Channel, Serial 116221, by Hydraulic Design and Products Co., which had a 6-in.-wide passage, 8 ft long and which utilized a sluice gate and weir for flow control (see sketch in Ref. 12). This basic equipment was altered in three ways. First, a flow straightening system was installed at the upstream end. Second, 2.50-in.-diam holes were drilled through the bottom and one side of the channel 27 in. downstream of the flow straightener to permit insertion of the injection chambers. Third, the bottom and one side of the channel were covered with $\frac{1}{8}$-in.-thick white plastic sheets that were ruled with 1-in. squares in black paint.

Injection System

The injectant fluid which was water dyed with equal parts of green and red food coloring, 2 oz/gal, was driven from an insulated aluminum heating vessel by means of air pressure (10–15 psig). The heating was accomplished electrically and the flow rate was controlled by a needle valve.

The injection chambers, machined out of solid lucite, were inserted through the channel wall from the outside. Each chamber had a $\frac{9}{16}$-in. flat bottomed hole drilled to within $\frac{1}{8}$ in. of the surface facing the flow. A $\frac{1}{16}$-in. hole was then bored through to form the injection port. Copper-constantan thermocouples were provided to measure the temperature of the injectant and freestream fluids.

Test Conditions

The weir was set so that the water depth of the main flow at the injection point was 4.8 in. The physical dimensions of and flow properties in the channel were such that fully developed flow could not occur. The flow conditions suggested that the Reynolds number based on the length along the channel measured from the flow straightener was 6.8×10^4 at the injection station. This implies a laminar flow and an estimated boundary-layer thickness of approximately 0.5 in.

The tests were conducted for the injection of the jet into the main flow in two ways. The first was a vertical injection from the channel floor, and the second was an oblique injection, 40° above the horizontal, from the channel wall. The results of these tests complement those published by the authors[13] where the jet was oriented to inject laterally from the channel wall. The present injection processes were observed with the jet temperature the same as the freestream temperature ($T_i = T_\infty$) and with it 45°F warmer ($T_i = T_\infty + 45°F$). The values of Re_{d_i} corresponding to these injection temperatures were 1319 and 2030, respectively, with $VR = 9$ and were 4333 and 6669, respectively, with $VR = 29$.

Results

An example of the type of photographic results obtained during this investigation for both vertical and oblique injection into the main flow can be seen in Figs. 1 and 2 where the injectant and freestream fluid temperatures are the same. The freestream is flowing from right to left.

Vertical injection

The effect of increasing jet injection velocity is illustrated in Fig. 1 for the vertical injection case, where an increase in the jet injection velocity results in further penetration of the jet flow into the mainstream.

The photographs indicate that for the highest injection velocity the area occupied by the jet fluid begins to grow immediately after injection, and that this growth continues as the jet structure bends over under the influence of the freestream flow. At some point downstream of the injection station, the jet flow becomes parallel to the freestream flow and subsequently becomes completely disorganized and random. The turbulent nature of the jet injection process can be seen in the very irregular boundary of the jet which is an indication of large-scale eddies in the flow. The basic characteristics of the injection process are the same for the lowest injection velocity ($VR = 9$) except that the jet fluid penetrates a discrete distance into the freestream flow before beginning to spread and bend over. This indicates that the jet flow is laminar at the injection point and undergoes transition to turbulent flow at some point along the trajectory. This laminar flow situation results because the Reynolds number of the jet flow at the injection point, as dictated by test conditions, is less than the critical value of Reynolds number (≈ 2300). The highest injection velocity in Fig. 1 results in a jet-exit Reynolds number that is larger than the critical value thus allowing the jet flow to begin spreading immediately after injection.

The addition of heat to the injectant resulted in no discernible effects on jet trajectory for the injection velocities tested, but did cause the jet flow to spread at a slightly greater rate immediately after injection. At first glance, the failure of the warmer jet fluid

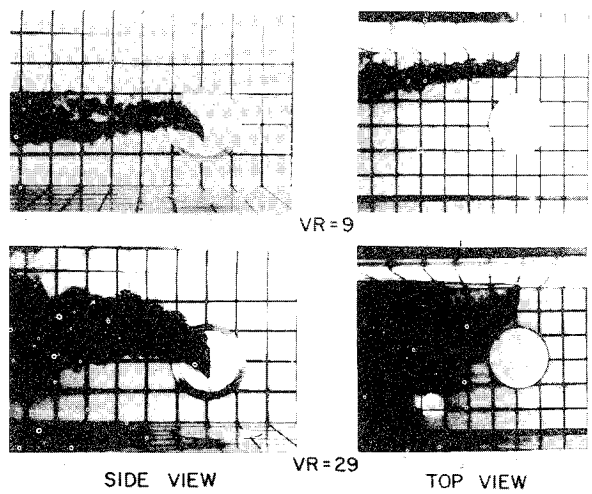

Fig. 2 Photographs of oblique injection for several injection velocities; $T_i = T_\infty$.

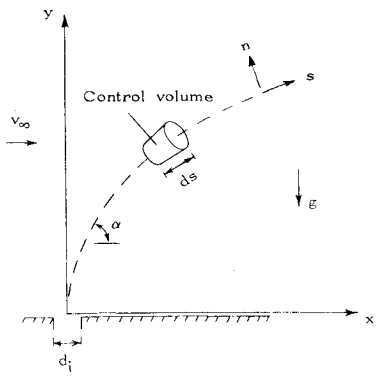

Fig. 3 Schematic representation of jet control volume and center-line trajectory.

to show some tendency to rise might be disconcerting. The fact, however, that water density is relatively insensitive to temperature changes and that the jet flow cools rapidly along the trajectory, a result to be shown in the next section of the paper, precludes the existence of large buoyancy forces.

Oblique injection

The effect of increasing injection velocity of the unheated jet injecting obliquely into the main flow (see Fig. 2) is similar to that discussed for the vertical injection process. The tests showed that increasing the injectant temperature caused a larger rate of spreading of the jet flow for $VR = 9$ and resulted in a higher trajectory for $VR = 29$.

That the oblique injection condition demonstrates an effect of injectant temperature on trajectory, while the vertical injection condition demonstrates no effect, draws attention to a subtle difference between oblique injection and vertical injection which has to do with the orientation of the vortices in the respective jet flows. Keffer and Baines[5] describe how a pair of counter-rotating vortices is formed in the rear portion of a jet injecting into a crossflow. For the vertical and lateral[13] injection processes, the jet is injected perpendicularly through the boundary layer on the adjacent wall. The vortices formed during the injection process are located symmetrically on either side of the jet center line, such that a line drawn between the vortex centers would be perpendicular to the plane of the trajectory. This description does not remain completely accurate for oblique injection through the boundary layer. From observations of the oblique injection experiments, it appeared as if the vortex pair was "twisted" immediately after injection so that the pair was oriented in a manner similar to the vortices generated by a lateral injection, that is, where the line between the vortex centers is vertical. Although detailed measurements are necessary to validate these comments, it is believed that the observed effects of injectant temperature on jet trajectory for the oblique and vertical injection conditions are the result of differences in vortex formation in the jet flows.

Theoretical Development

In this section we will be concerned with the development of a theoretical method for predicting some of the primary flow properties of submerged heated effluents discharging into a waterway.

One approach that has shown a great deal of promise for our use considers the effluent as a submerged turbulent jet flow injecting into a moving water system where the fluid motion of the jet is described from the point of discharge in a Lagrangian framework. (See coordinate system in Fig. 3.) This procedure uses the control volume concept to monitor the flow processes in the jet and integral techniques to yield the average, or mean, jet properties along the trajectory. Several investigators[9,10,13] have recently used this method to estimate jet trajectories in the proximity of the injection point ($s/d_i \leqq 10$), but because of certain assumptions in their theories, these studies are not suitable for providing realistic trajectory information farther downstream. The present investigation relaxes many of the assumptions used in these studies and attempts to account for natural flow phenomena not considered heretofore, such as turbulence and heat transfer.

Mass

The differential form of the mass continuity equation may be written as

$$E = (d/ds)(\rho A v) \tag{1}$$

which represents the mass flow per unit length entrained through the sides of the control volume. Inclusion of this entrainment process in an analysis of the type considered in this paper is important, not only because of its influence on jet trajectory, but also because of its role in determining heat loss from the jet fluid.

Because of the complicated nature of analytically predicting the entrainment function, the experimental data generated by Keffer and Baines[5] for an air jet were used to estimate this property of the water jet injection process of the present study. Equation (2) represents the entrainment parameter in functional form, where the entrainment coefficient (E^*) was obtained from measurements of mass flux along the jet axis[5]

$$E = (A/C)\rho_{\alpha} E^*(v - v_{\alpha}) \tag{2}$$

An empirical expression was obtained for E^* for use in the present mathematical model and is presented in Ref. 12.

n-Momentum

The n-momentum equation represents the balance of forces acting perpendicular to the jet trajectory and is obtained by taking the n components of the vector quantities in the momentum integral equation.

$$\rho A v^2/R = C_D q_{\alpha} h \sin^2\alpha - gA(\rho - \rho_{\infty})\cos\alpha - Ev_{\infty}\sin\alpha \tag{3}$$

The centrifugal force results from the jet fluid having a mass, a velocity, and following a curved path, while the buoyancy force results from a difference in density (i.e., temperature) between the jet and freestream fluids. The integrated shear-stress tensor, which includes surface pressure distribution over the control volume, yields the total drag force on the jet due to the blockage of the freestream flow; this is postulated to be the drag on an equivalent "solid" cylindrical jet shape inclined at an angle to the freestream flow. The remaining term in Eq. (3) accounts for the net influx of momentum into the control volume.

At this stage of the development, the approach used in previous studies[8-10,13] has been to assume the area growth of the jet along the trajectory, the rate of growth being based on experimental measurements where $s/d_i \leqq 10$. The area growth can be obtained by assigning a certain shape for the jet cross section and by allowing the jet width to grow at a specified rate. The expression for mass flow in the jet is used to eliminate velocity in the n-momentum equation, and the resulting expression is integrated to obtain a solution for the jet trajectory. Typical results obtained by this procedure are presented in Fig. 4 for a jet with an elliptical cross-sectional shape and are compared with experimental data[13] acquired from photographs.

Comparison of the assumed cross-sectional areas with the values obtained from experiments shows that the two are in reasonable agreement in the proximity of the jet exit, but that the values diverge as the jet proceeds downstream, the measured areas indicating a much more rapid rate of jet growth than the assumed values. This trend is reflected in the trajectory information where good agreement between the predicted and experimental trajectories is noted in the initial region after jet injection, but poor agreement occurs farther downstream.

The reason for this poor agreement in trajectories is due to the fact that the theoretical jet velocity begins to increase at some point on the trajectory, as illustrated by the velocity deficit curve

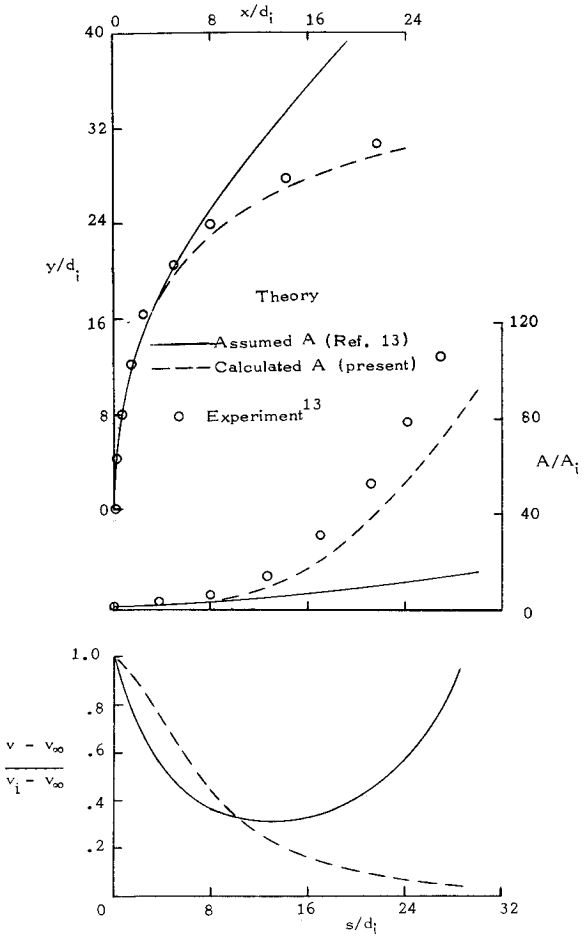

Fig. 4 Effect of area growth assumption on theoretical jet flow properties; $VR = 18$; $T_i = T_\infty$.

in the figure. The reader is aware, of course, that as long as the jet injection velocity is greater than the freestream velocity, then the jet velocity will decrease continuously along the trajectory, eventually approaching the freestream velocity value far downstream. These erroneous trends for the theoretical jet velocity can be traced directly to the use of an assumed area growth.

From these remarks, it is obvious that an alternative approach be considered such that the jet cross-sectional area is permitted to be an unknown in the governing equations. In order to do this, it is necessary to have another equation; the equation expressing conservation of momentum along the trajectory satisfies this need. By using this additional momentum equation, a more natural description of the jet flow properties is obtained as is illustrated in Fig. 4.

Although the area assumption is to be discarded, it is still necessary to provide information concerning the width of the jet in order to calculate the drag and shear stress terms in Eqs. (3) and (4), respectively. The approach used in previous studies has been to assume the growth of the jet width along the trajectory; another approach is to specify a shape for the jet cross section, and use this with the computed area to calculate the jet width. The latter approach is utilized herein.

Keffer and Baines[5] have shown that the typical "kidney" shape of the jet cross section remains approximately the same with increase in s. For the present study, this shape is assumed to be elliptical with a ratio of major to minor axes of 5 to 1 (after Abramovich[8]) the major axis being the jet width. The value of C_D associated with this shape is taken to be 1.6 in keeping with the equivalent "solid" body argument. It is noted that Wooler et al.[10] used a value of 1.8 in their analysis while Abramovich[8] used 3.0, a value which was pointed out in Ref. 9 as being totally unrealistic.

s-Momentum

The s-momentum equation is obtained by taking the s components of the vector quantities in the momentum integral equation. The resulting expression, Eq. (4), represents a balance between the rate of change of jet momentum and the forces on the jet due to changes in mean jet pressure, to buoyancy, to entrainment of ambient fluid into the jet, and to shear stress between the jet and freestream fluids

$$\partial(\rho A v^2)/\partial s = -A\partial\bar{p}/\partial s - gA(\rho-\rho_\infty)\sin\alpha + Ev_\infty\cos\alpha - \pi h\tau \quad (4)$$

To evaluate the static pressure gradient along the trajectory ($\partial\bar{p}/\partial s$), the assumption is made that the freestream static pressure field around the jet perimeter imposes itself on the jet flow. For the present case where the jet structure is considered as an elliptical cylinder inclined at an angle to the freestream flow, there are large variations in the freestream pressure field due to the blockage effect that the jet has on the freestream flow. Some idea of the static pressure variation around the perimeter of a jet cross section, idealized as a circular cylinder, can be obtained by observing experimental pressures.[14] An estimate of this variation was obtained for use in the theory by assuming that the pressures on the front of the cylinder ($0 \leqq \theta \leqq \pi/2$) are specified by potential flow theory, and the pressures on the back of the cylinder ($\pi/2 < \theta < \pi$) are equal to the freestream pressure. Although the pressure field resulting from the turbulent jet injection process is very complicated and does not lend itself to be categorized in this simple a fashion, the procedure is adequate for use in the present mathematical model.

The local surface pressure is used in the expression

$$\bar{p} = \int_0^\pi p\,d\theta \Big/ \int_0^\pi d\theta \quad (5)$$

to obtain the average static pressure acting on the cylinder. Performing the integrations in Eq. (5) we obtain

$$\bar{p} = p_\infty - \tfrac{1}{2}q_{\infty_n} \quad (6)$$

where it is recalled that q_{∞_n} is the freestream dynamic pressure normal to the trajectory. This equation implies that the average static pressure on the jet cross section is less than the freestream static pressure but approaches p_∞ as the q_{∞_n} approaches zero. $\bar{p}$ can be differentiated with respect to s to get

$$\partial\bar{p}/\partial s = -q_\infty \sin\alpha\cos\alpha\, d\alpha/ds \quad (7)$$

For the present case of a jet injecting into a crossflow, the viscous shear stresses in the s direction are proportional to the differences between the jet velocity and the freestream velocity component tangent to the jet flow. These shear stresses can be approximated by

$$\tau = \rho(\nu+\varepsilon)\frac{\partial U}{\partial n} \quad (8)$$

where U represents a velocity in the s direction, and $\partial U/\partial n$ represents the gradient of that velocity in the n direction. The kinematic viscosity will be neglected for the present study since, for turbulent mixing flows, it is small compared to the virtual (eddy) viscosity.

The method used to estimate the eddy viscosity for this jet injection process is based on Prandtl's hypothesis[14] and is valid only for free turbulent flows. The viscosity is represented by

$$\varepsilon = \beta b(U_{\max} - U_{\min}) \quad (9)$$

where β is an empirical constant and b is the width of the mixing zone. The minimum velocity in this expression is defined as the freestream velocity component tangent to the direction of jet flow, while the maximum velocity is defined as the mean jet velocity in order to be compatible with previous mean flow assumptions. The velocity gradient is approximated by

$$\partial U/\partial n = (U_{\max} - U_{\min})/b = (v - v_\infty\cos\alpha)/b \quad (10)$$

so that the shear stress can be written as

$$\tau = \rho\beta(v - v_\infty\cos\alpha)^2 \quad (11)$$

Incorporating the pressure gradient term, Eq. (7), and the

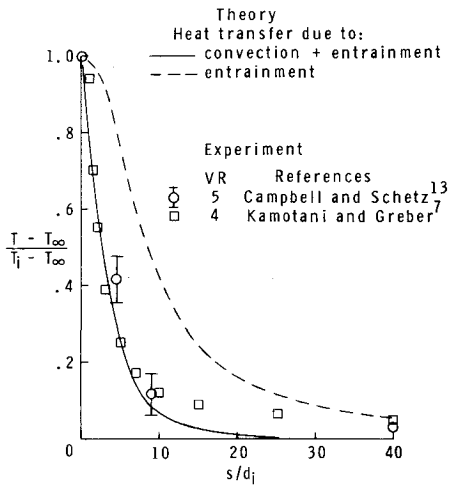

Fig. 5 Variation of jet temperature deficit with distance along the trajectory for heated injection process ($T_j > T_\infty$).

shear stress term, Eq. (11), into Eq. (4) yields the final form of the s-momentum expression:

$$(\partial/\partial s)(\rho A v^2) = q_\infty A \sin\alpha \cos\alpha \, d\alpha/ds - gA(\rho - \rho_\infty)\sin\alpha + Ev_\infty \cos\alpha - \pi h \rho \beta (v - v_\infty \cos\alpha)^2 \quad (12)$$

In order to obtain an estimate for the empirical constant β, it is necessary to rely on existing information related to less complex turbulent flows than the jet injection process considered in the present study. The procedure used here is to estimate β at the beginning of the injection by assuming that a two-dimensional freejet boundary exists between the jet velocity and the freestream velocity component tangent to the jet flow. Schlichting's description of a free jet boundary[14] is used to obtain the expression

$$\beta = 0.00137/c\lambda \quad (13)$$

where c is the rate of spread of the jet flow, taken to be a constant (0.32) for this study.

The velocities U_{max} and U_{min} in the analysis of the free jet boundary are considered to be constant as the jet proceeds away from the point of initial flow interaction. In the present situation, U_{max} and U_{min} continuously change as the jet flow is decelerating and bending over. Accordingly, the velocity parameter used in Ref. 14 is redefined as

$$\lambda = (v - v_\infty \cos\alpha)/(v + v_\infty \cos\alpha) \quad (14)$$

which forces β to be dependent on the local velocity conditions along the trajectory. It is noted that at the injection point $\lambda = 1.0$. This representation is used until β attains the following value prescribed by a circular freejet analysis[14]:

$$\beta = 0.00217/c \quad (15)$$

This description of β is assumed to apply for the remainder of the jet trajectory.

Heat Energy

Up to now we have discussed only the mass and momentum aspects of the jet injection process; however, since the present investigation is concerned with heated discharges, it is desirable to also consider some of the thermal characteristics. In particular, it is advantageous to determine the change in mean jet temperature resulting from the penetration of the jet into the crossflow. This can be accomplished by monitoring the heat loss from the control volume, this heat loss being considered in the present study as resulting from two different types of heat-transfer mechanisms.

The first type of heat-transfer mechanism pertains to the reduction in energy content per unit volume ($\rho c_p T$) of the jet fluid due to the entrainment of freestream fluid at a different energy level ($\rho c_p T)_\infty$. Applying this concept to the control volume results in the expression

$$(mc_p T)_2 = (mc_p T)_1 + m_e (c_p T)_\infty \quad (16)$$

where $(mc_p T)_1$ represents the energy level in the control volume that would exist if there were no entrainment, and $(mc_p T)_2$ represents the equilibrium energy level resulting from the complete mixing of the jet and entrained fluids. Since the specific heat (c_p) of water is fairly insensitive to temperature changes, the various specific heats in Eq. (16) are assumed to have the same value.

Forced convection, the second type of heat-transfer mechanism being considered, results when the freestream flows around the heated jet fluid and extracts heat energy from the jet in the process. This heat transfer is analogous to the forced convection over a heated cylinder, where the cylinder is cooled by the fluid flowing normal to the cylinder's axis. To be consistent with our previous arguments, the convective heat transfer is estimated by considering the jet structure as a cylinder inclined at an angle to the freestream flow.

Eckert and Drake[15] suggest the following expression for estimating an average Nusselt number:

$$Nu_d = 0.43 + 1.11\, F(Re_d)^\gamma (Pr)^{0.31} \quad (17)$$

where Prandtl number is chosen as 1.0 for simplicity. The Reynolds number is defined using the "effective" diameter of the jet as the reference length and the freestream velocity component perpendicular to the jet axis as the reference velocity, so that Nusselt number will be sensitive to the local flow changes as the jet penetrates into the crossflow. The Reynolds number is thus

$$Re_d = v_\infty d \sin\alpha / \nu_\infty \quad (18)$$

The values of Re_d occurring in the present experiment suggest the selection of $F = 0.45$ and $\gamma = 0.50$ for use in Eq. (17).

The definition of Nusselt number is used to obtain the average film heat-transfer coefficient, which yields the rate of heat loss from the jet fluid,

$$Q = \bar{h} A (T_\infty - T) \quad (19)$$

An example of the temperature results obtained when these two heat-transfer mechanisms are incorporated into the analytical model is presented in Fig. 5, where the theoretical calculations were made with the same injection conditions as Ref. 13. The trend of temperature decrease along the trajectory[13] is adequately estimated by the theory, the predicted mean temperature values falling below the measured maximum temperatures. These results are substantiated by the temperature data for an air injection process measured by Kamotani and Greber.[7] The theoretical temperatures obtained by considering only the effects of entrainment are presented to demonstrate the relative magnitudes of the two types of heat-transfer mechanisms. Convection is seen to be the dominant mechanism for determining temperature loss in the early stages of the jet injection process, while the effects of entrainment become dominant as the jet proceeds downstream.

Solution Procedure

An iterative method is employed to obtain a solution of the highly nonlinear governing differential equations at specific locations along the jet trajectory. The basic procedure is to solve Eq. (12) for the s momentum of the control volume, where the coefficients in that equation are estimated using the flow property values obtained from the solution at the previous location on the trajectory. The s momentum is used in conjunction with the continuity equation to provide an update on v, and the heat loss from the control volume is calculated to provide new estimates for ρ and T. The current flow property values are then used in the coefficients of the n-momentum equation, Eq. (3), to obtain a solution for $d\alpha/ds$, from which α is acquired using a Taylor series expansion. The most recently calculated flow property values are used to iterate back through the governing equations, only a few iterations being required to yield satisfactory results. Incremental values of x and y are obtained from the final value of trajectory slope and from the assigned value for ds. These increments are added to the coordinates of the previous location on the trajectory to obtain the new x, y trajectory coordinates. This procedure is repeated at each incremental "step" along the trajec-

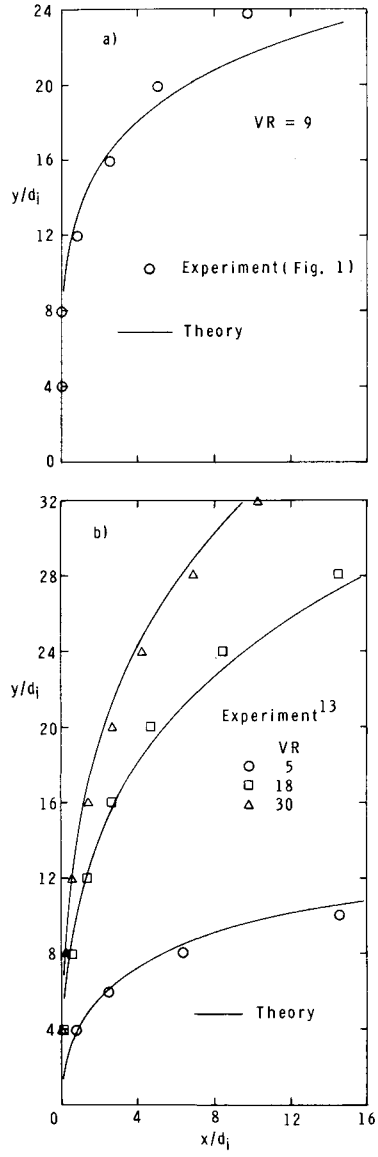

Fig. 6 Experimental and theoretical jet trajectories for a range of injection velocities; $T_i = T_\infty$.

tory to provide a solution for the trajectory and cross-sectional area of the jet flow, as well as the jet flow properties of mass, momentum, velocity, and temperature.

Examples of the results obtained by the present effort to theoretically model the jet injection process are presented in the following section.

Discussion

Experimental trajectory data obtained from several investigations are compared with the present theory in Figs. 6 and 7 and show the paths of the jet as it penetrates into the main flow after being injected perpendicular to the freestream direction. The data in Fig. 6 were acquired from photographs of water injection and represent the path of the approximate center line of the jet flow, while the experimental information in Fig. 7 was obtained from hot-wire measurements of air injection and represents the path of the maximum velocity in the jet flow. The theory provides good estimates of jet trajectory for the range of injection conditions shown. It should be noted that the experimental results of Figs. 6b and 7 are for completely turbulent jet flows, whereas the data in Fig. 6a represent a jet flow that is partially laminar (see Fig. 1). In order to estimate the trajectory

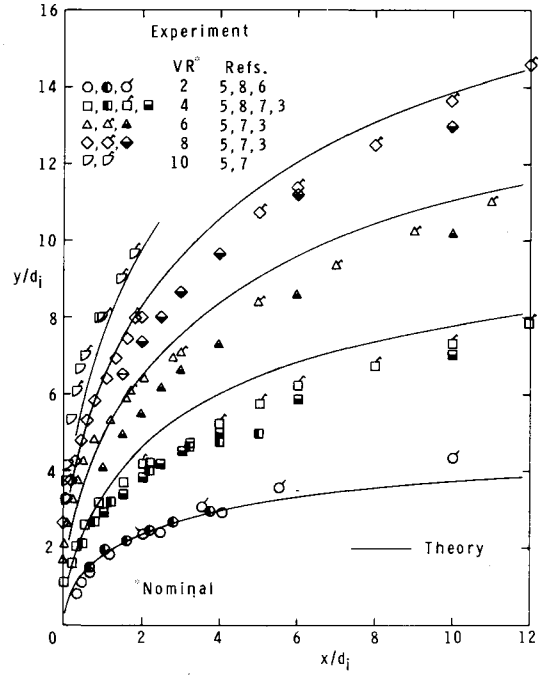

Fig. 7 Experimental and theoretical air-jet trajectories for a range of injection velocities; $T_i = T_\infty$.

for the mixed flow situation the theory was adjusted to account for the initial laminar portion of the jet flow by assuming that the jet begins its turbulent growth at a point specified in the photograph of Fig. 1 ($y/d_i \approx 8$).

Examples of some of the theoretical flow properties obtained in the process of solving for the trajectories are presented in Figs. 8 and 9. The cross-sectional area of the jet continually increases as the jet flow continues along the trajectory (Fig. 8), the largest rates of area growth generally occurring for the largest injection velocities. Predicted jet areas resulting from injection with $VR = 30$ are compared with experimental areas obtained from photographic data[13] for the same injection condition. The experimental areas were obtained by assuming the jet cross-sectional shape to be a 5:1 ellipse.

As the area occupied by the jet fluid grows with increase in s, the jet velocity correspondingly decays and eventually approaches the freestream velocity value (Fig. 9). The trend for velocity decay is similar for all the injection velocities, although the respective values of v/v_i are proportionately lower for the

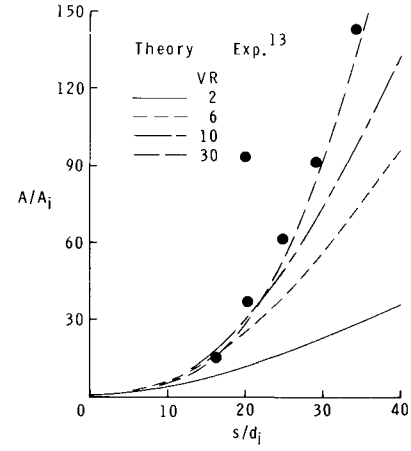

Fig. 8 Variation of jet cross-sectional area with distance along the trajectory for a range of injection velocities; $T_i = T_\infty$.

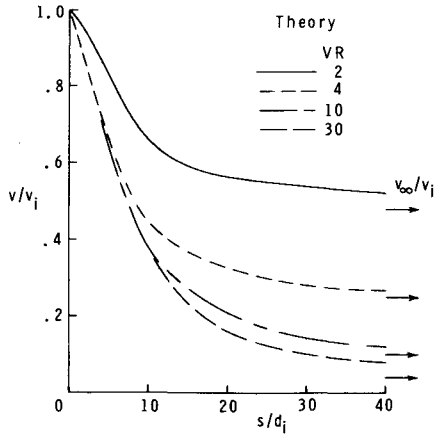

Fig. 9 Variation of theoretical jet velocity with distance along the trajectory for a range of injection velocities; $T_j = T_\infty$.

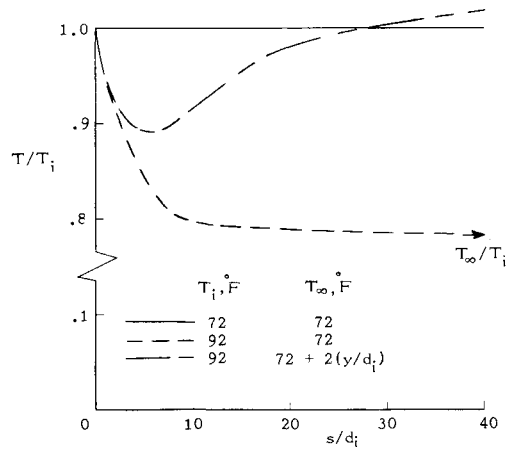

Fig. 11 Effect of freestream temperature nonuniformity on theoretical jet temperature; $VR = 5$.

larger injection velocities. This trend results because the jet velocity ratio must approach smaller values of v_∞/v_j (depicted by the arrows) as VR increases. Variations of theoretical mass and momentum flux in the jet with distance along the trajectory are presented in Ref. 12.

One advantage of the present theory is its flexibility for investigating different parameters which affect the trajectory and flow properties of the injected jet. Not the least important of these parameters is the freestream velocity and temperature field into which the jet is injected. Up until now the freestream velocity and temperature have been assumed constant, but the next few figures will demonstrate some of the effects resulting from relaxing these restrictions.

For the purpose of this illustration, the nonuniform freestream velocity field, Fig. 10, is assumed to have a boundary-layer type of velocity distribution in the y-direction and to be independent of x. A Kármán-Pohlhausen velocity function[15] is described from the injection surface to the point where $y/d_j = 8$. At larger values of y/d_j the velocity is assumed to be constant having the same value as the v_∞ used for the uniform freestream velocity case. Injecting into the nonuniform freestream velocity field results in further penetration by the jet into the crossflow than injection into the freestream with the uniform velocity field. Coincident with this, the jet velocity decay was essentially unaffected, while the jet cross-sectional area and momentum were less at any given distance along the trajectory.

Injecting a jet with initial temperatures of 72°F and 92°F into a freestream flow having uniform temperature and velocity fields results in the temperature curves shown in Fig. 11. Although the heated jet flow might be expected to rise above the trajectory for the unheated case, the rapid heat loss from the jet reduces the influence of buoyancy and hence results in no change in the trajectory.[12] This result agrees with the experimental observations presented earlier in the paper and with the measurements made by Kamotani and Greber.[7] As noted in the figure, the temperature for the heated jet decreases along the trajectory until it reaches the freestream temperature value (T_∞/T_j).

A linear temperature gradient is used to demonstrate the effect of injecting a heated jet vertically into a freestream flow having a nonuniform temperature field. The freestream temperature at the injection surface is equivalent to the value used for the uniform freestream temperature case. Injection of the heated jet into the freestream flow with a temperature gradient results in a trajectory similar to that obtained by injecting the heated jet into the uniform temperature field.[12] There is a definite difference, however, in the jet temperature curves resulting for these two injection conditions, where the nonuniform T_∞ situation results in higher jet temperatures because of the larger values of T_∞ that the jet flow "sees" as it penetrates into the crossflow. Heat is initially lost from this jet flow until a point is reached on the trajectory where a heat gain is experienced.

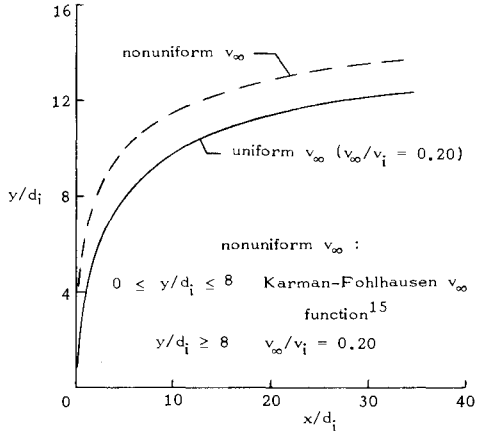

Fig. 10 Effect of freestream velocity nonuniformity on theoretical jet trajectory; $T_j = T_\infty$.

Concluding Remarks

Experimental results for both the vertical and oblique injection conditions showed that increasing jet injection velocity resulted in further penetration of the jet flow into the mainstream. Addition of heat to the injectant caused a slightly greater rate of spreading of the jet fluid near the injection point. Increasing injectant temperature had no discernible effect on jet trajectory for the vertical injection condition but resulted in a higher trajectory for oblique injection with the largest injection velocity.

A theory was developed by using an integral method, which accounted for natural fluid mechanisms such as turbulence, entrainment, buoyancy, and heat transfer, to obtain the conservation equations of the jet flow. Solving these equations simultaneously yielded predictions of jet trajectory and area growth that agreed well with experimental results, and thus demonstrated the usefulness of the theory for estimating the locaton and size of the thermal plume with respect to the discharge point.

Unlike previous studies which assumed a specific cross-sectional area growth for the jet, the present investigation obtained the jet cross-sectonal area in the process of solving the governing equations. Because of this, the present theory provided better estimates for the trajectory and area growth of the jet and allowed a prediction for various jet flow properties, such as velocity and momentum, to be obtained.

Realistic estimates of temperature in the jet fluid were obtained by accounting for heat losses in the jet flow due to forced con-

vection and to entrainment of freestream fluid into the jet. Forced convection was seen to be the dominant heat-transfer mechanism during the early stages of the jet injection process, while the effects of entrainment became dominant as the jet penetrated further into the freestream flow.

References

[1] Edinger, J. E. and Geyer, J. C., "Heat Exchange in the Environment," Prepared for Edison Electric Inst. Research Project No. 49, EEI publication 65-902, June 1965, Dept. of Sanitary Engineering and Water Resources, The Johns Hopkins Univ., Baltimore, Md.

[2] Mahgary, Y. S. E., "Thermal Diffusion of the Warm Water of Power Plants into a Sea Basin," *Journal of Environmental Sciences*, Nov./Dec. 1971, pp. 20–23.

[3] Jordinson, R., "Flow in a Jet Directed Normal to the Wind," R. & M. No. 3074, 1958, British Aeronautical Research Council.

[4] Margason, R. J., "The Path of a Jet Directed at Large Angles to a Subsonic Free Stream," TN D-4919, Nov. 1968, NASA.

[5] Keffer, J. F., and Baines, W. D., "The Round Turbulent Jet in a Cross-Wind," *Journal of Fluid Mechanics*, Vol. 15, Pt. 4, 1963, pp. 481–496.

[6] Ramsey, J. W., "The Interaction of a Heated Air Jet With a Deflecting Flow," Ph.D. thesis, June 1969, Univ. of Minnesota, Minneapolis, Minn.

[7] Kamotani, Y. and Greber, I., "Experiments on a Turbulent Jet in a Cross Flow," CR-72893, June 1971, NASA.

[8] Abramovich, G. N., *The Theory of Turbulent Jets*, The MIT Press, Cambridge, Mass., 1963, pp. 541–553.

[9] Schetz, J. A. and Billig, F. S., "Penetration of Gaseous Jets Injected Into a Supersonic Stream," *Journal of Spacecraft and Rockets*, Vol. 3, No. 11, Nov. 1966, pp. 1658–1665.

[10] Wooler, P. T., Burghart, G. H., and Gallagher, J. T., "Pressure Distribution on a Rectangular Wing With a Jet Exhausting Normally Into an Airstream," *Journal of Aircraft*, Vol. 4, No. 6, Nov.-Dec. 1967, pp. 537–543.

[11] *Analysis of a Jet in a Subsonic Crosswind*, NASA SP-218, Sept. 1969.

[12] Campbell, J. F. and Schetz, J. A., "Flow Properties of Submerged Heated Effluents in a Waterway," AIAA Paper 72-79, San Diego, Calif., 1972.

[13] Campbell, J. F. and Schetz, J. A., "Penetration and Mixing of Heated Jets in a Waterway With Application to the Thermal Pollution Problem," AIAA Paper 71-524, New York, 1971.

[14] Schlichting, H., *Boundary-Layer Theory*, 6th ed., McGraw-Hill, New York, 1968, pp. 681–707.

[15] Eckert, E. R. G. and Drake, R. M., Jr., *Heat and Mass Transfer*, 2nd ed., McGraw-Hill, New York, 1959, pp. 139, 239–243.